

Properties of chord length distributions across ordered and disordered packing of hard disks

David Guéron and Alain Mazzolo

CEA-Centre d'Etudes de Saclay, DEN/DM2S/SERMA/LEPP, 91191 Gif-sur-Yvette, France

(Received 1 August 2003; published 24 December 2003)

Chord length distributions across packings—random or not—of equal hard disks have a universal divergence which is proportional to n_c/\sqrt{l} for small chords, where n_c is the mean number of contacts. A similar behavior is derived for a population of polydisperse disks. Monte Carlo simulations across various kinds of regular and random packings are in full agreement with the theoretical predictions.

DOI: 10.1103/PhysRevE.68.066117

PACS number(s): 02.50.-r, 05.10.-a, 81.05.Rm

I. INTRODUCTION

Purely two-dimensional physical phenomena such as clustering of bacteria or adsorption of monomolecular layers of large molecules on surfaces are modeled by two-dimensional disk packings [1]. Information regarding such systems can be obtained by looking at the chord length distribution (CLD). Indeed, the study of chord length distributions across various kinds of two-dimensional geometric shapes, including binary stochastic mixtures, is a topic of great interest in many research fields ranging from image analysis [2] to neutronics [3].

The aim of this paper is to present the behavior of the CLD for small chords across an arrangement of hard disks in which the particles are in contact with one another, following a geometric argument of Pomeau [4]. As a first step, this behavior is derived for packings of equal disks and then extended to the general case of disks of arbitrary size. Monte Carlo simulations across several regular disk packings as well as various random disk packings, including ballistic deposition model, illustrate our point.

II. MONODISPERSE DISKS

In a couple of papers Pomeau [4] and Pomeau and Serra [5] consider a packing of hard spheres and show that measurements in \mathbb{R}^2 give direct access to the coordination number n_c of spheres in \mathbb{R}^3 . More precisely, the authors mentioned above relate n_c to the distribution function of the small chords between the neighboring disks of a uniformly oriented two-dimensional section of the packing [Eq. (3) in Ref. [5]]. In the following, using a likewise geometric argument, we derive the relation between n_c (for $n_c \neq 0$) and the CLD for small distance for a packing of hard disks. Note that the special packings considered in the present paper in which the particles are in contact with one another includes the packings referred to “jammed” packings (see Ref. [6] for a precise definition of a jammed packing and Ref. [7] for examples of such packings). In fact, most of the packings presented hereafter are jammed packings, however our calculations are not limited to such packings and an example of unjammed random packing is presented at the end of Sec. IV.

Let us consider two touching hard disks of same radius R in the plane as shown in Fig. 1.

In the present paper, the chords we consider are the chords generated between two touching disks by a random

straight line. In a plane, a straight line can be represented by its polar coordinates ρ and θ as shown in Fig. 2.

An important result of geometric probability is that, up to a constant, the only measure for sets of straight lines which is invariant under the group of motions (i.e., translations and rotations) is the uniform measure $dM = d\rho d\theta$ [8,9]. Here, for the needs of the paper, θ is sampled uniformly over $[-\pi/2, \pi/2]$ while ρ is sampled uniformly over $[-R, R]$. Consequently, the density probability measure of random lines across a disk of radius R is

$$dM = \frac{d\rho}{2R} \frac{d\theta}{\pi} \quad \text{with } \rho \in [-R, R] \text{ and } \theta \in [-\pi/2, \pi/2], \quad (1)$$

where we notice that the denominator of Eq. (1) is the perimeter of the disk, which is precisely the measure of the set of straight lines intersecting the disk [8]. Since the measure is invariant under rotation and translation, it is always possible to chose the X axis as the axis between the two disks' center and the origin at the center of a disk, as shown in Fig. 1. Now, given a fixed (small) distance l and an angle θ , the chords smaller than l are generated by lines of polar coordinates (ρ, θ) , where $h_1 \leq \rho \leq h_2$, h_1 and h_2 being the two radii such that the length of the generated chord is l as illustrated by Fig. 1. From Fig. 1 we get, using the notation $\Delta h = |PQ| = h_2 - h_1$,

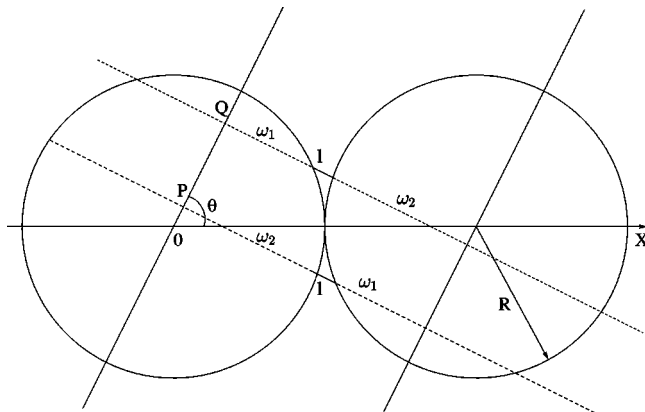


FIG. 1. Chords across two touching disks: all the chords smaller than l are supported by random lines that pass between P and Q ($h_1 = |OP|$ and $h_2 = |OQ|$).

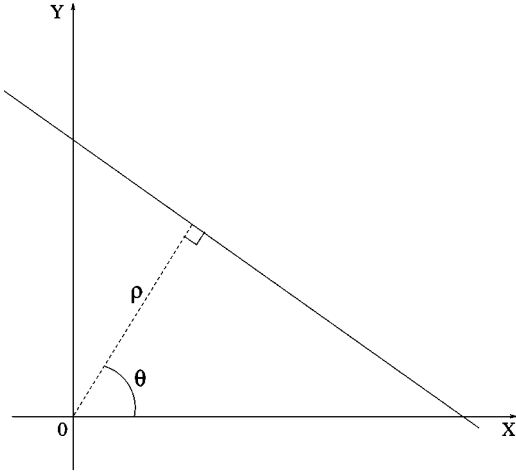


FIG. 2. Random line in the plane.

$$\begin{aligned}
 2R \cos \theta &= h_1 + (h_1 + \Delta h), \\
 2R \sin \theta &= \omega_1 + \omega_2 + l
 \end{aligned}
 \tag{2}$$

and

$$\begin{aligned}
 R^2 &= \omega_2^2 + h_1^2, \\
 R^2 &= \omega_1^2 + (h_1 + \Delta h)^2.
 \end{aligned}
 \tag{3}$$

Combining the two preceding couple of equations leads to

$$l = 2R \sin \theta - [\sqrt{R^2 - h_1^2} + \sqrt{R^2 - (2R \cos \theta - h_1)^2}].
 \tag{4}$$

After some algebra, Eq. (4) can be rewritten as a second-order equation

$$\begin{aligned}
 h_1^2 [16R^2 + 4l^2 - 16lR \sin \theta] &+ h_1 [32lR^2 \sin \theta \cos \theta \\
 - 8l^2R \cos \theta - 32R^3 \cos \theta] &+ l^4 - 8l^3R \sin \theta \\
 + R^2 l^2 [5 - 4 \cos^2 \theta] - 16lR^3 \sin \theta &+ 16R^4 \cos^2 \theta = 0,
 \end{aligned}$$

whose solutions, which are precisely h_1 and h_2 , can be easily obtained. However, the complicated exact solutions have little interest since one looks at the small chords only. In the limit of such chords

$$\begin{aligned}
 h_1 &= R \cos \theta - \sqrt{R} \sin^{3/2} \theta \sqrt{l} + \frac{1}{8\sqrt{R}} [1 + 4 \cos^2 \theta] \sin^{1/2} \theta l^{3/2} \\
 &+ O(l^{5/2}),
 \end{aligned}$$

$$\begin{aligned}
 h_2 &= R \cos \theta + \sqrt{R} \sin^{3/2} \theta \sqrt{l} - \frac{1}{8\sqrt{R}} [1 + 4 \cos^2 \theta] \sin^{1/2} \theta l^{3/2} \\
 &+ O(l^{5/2}),
 \end{aligned}$$

and

$$\begin{aligned}
 \Delta h = h_2 - h_1 &= 2\sqrt{R} \sin^{3/2} \theta \sqrt{l} - \frac{1}{4\sqrt{R}} [1 + 4 \cos^2 \theta] \sin^{1/2} \theta l^{3/2} \\
 &+ O(l^{5/2}).
 \end{aligned}$$

For disks of radius of the order of unity (as it will be the case in our Monte Carlo simulations), the coefficient of $l^{3/2}$ in the expansion of Δh is of the same order as the one of $l^{1/2}$. We can therefore neglect the second term in our calculations. In order to obtain the measure $\tilde{M}(l)$ of the set of lines giving a chord less than l , we have to integrate the last quantity over θ which gives

$$\begin{aligned}
 \tilde{M}(l) &= \int_{-\pi/2}^{\pi/2} \Delta h d\theta = 2\sqrt{R} \sqrt{l} \int_{-\pi/2}^{\pi/2} |\sin \theta|^{3/2} d\theta \\
 &= 2\sqrt{\pi R} \frac{\Gamma\left(\frac{5}{4}\right)}{\Gamma\left(\frac{7}{4}\right)} \sqrt{l},
 \end{aligned}$$

where the symbol Γ denotes the Euler Γ function.

From now on, let us consider a packing of N equal disks whose mean number of contacts is n_c . For such a system, the measure $M(l)$ of all chords less than l is obtained by summing the last result over all the disks. By doing so each point of contact is twice taken into account so this amounts to the multiplication of Eq. (5) by $N n_c/2$, which gives

$$M(l) = n_c N \sqrt{\pi R} \frac{\Gamma\left(\frac{5}{4}\right)}{\Gamma\left(\frac{7}{4}\right)} \sqrt{l}.
 \tag{5}$$

In order to avoid difficulties regarding the normalization of the CLD, we also assume that each random line generates one chord or more precisely that the set of random lines that does not hit at least two disks has a null measure. Consequently, in the present paper we ignore infinite packings of dilute clusters where this hypothesis can be wrong. However, for a finite system the hypothesis of having a one to one correspondence between random lines and random chords clearly does not hold. The special case of two isolated touching disks is treated in Appendix A.

In order to obtain the distribution function of the chord length we have to normalize the preceding equation by the measure of the set of random lines generating a chord, which is $N(2\pi R)$. Thus we get

$$F(l) = \frac{n_c}{2\sqrt{\pi R}} \frac{\Gamma\left(\frac{5}{4}\right)}{\Gamma\left(\frac{7}{4}\right)} \sqrt{l},
 \tag{6}$$

and the density probability function $f(l)$ is

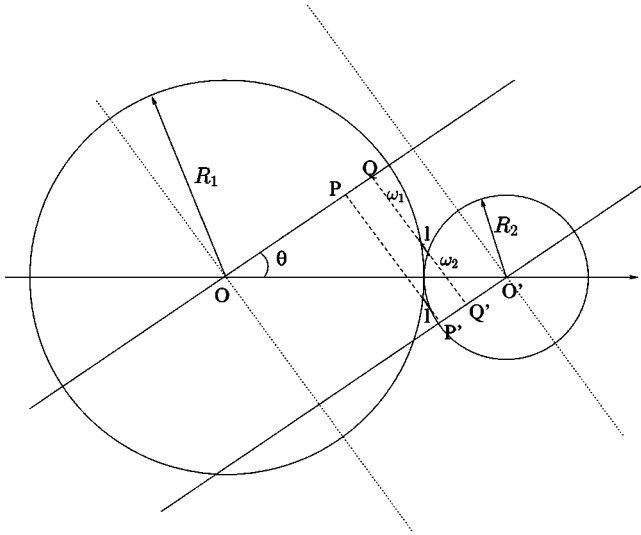


FIG. 3. Chords across two touching disks: all the chords smaller than l are supported by random lines that pass between P and Q ($h_1 = |OP|$, $h_2 = |O'Q'|$, and $\Delta h = |PQ| = |P'Q'|$).

$$f(l) = \frac{dF(l)}{dl} = \frac{n_c}{4\sqrt{\pi R}} \frac{\Gamma\left(\frac{5}{4}\right)}{\Gamma\left(\frac{7}{4}\right)} \frac{1}{\sqrt{l}}. \quad (7)$$

This probability density function, valid for small chords only, does not depend on any hypothesis regarding the regularity of the packing. This will be tested extensively through Monte Carlo simulations in Sec. IV.

III. POLYDISPERSE DISKS

In this section, we consider packings of disks of various radii keeping the hypothesis that a random line always generates a chord. For a couple of touching disks of radius R_1 and R_2 , Eqs. (2) and (3) become

$$\begin{aligned} (R_1 + R_2) \cos \theta &= h_1 + h_2 + \Delta h, \\ (R_1 + R_2) \sin \theta &= \omega_1 + \omega_2 + l \end{aligned} \quad (8)$$

and

$$\begin{aligned} R_1^2 &= \omega_1^2 + (h_1 + \Delta h)^2, \\ R_2^2 &= \omega_2^2 + h_2^2, \end{aligned} \quad (9)$$

where h_2 is the distance $|O'Q'|$ in Fig. 3.

Then relation, Eq. (4), is replaced by

$$\begin{aligned} l &= (R_1 + R_2) \sin \theta - \left[\sqrt{R_2^2 - h_2^2} \right. \\ &\quad \left. + \sqrt{R_1^2 - ((R_1 + R_2) \cos \theta - h_2)^2} \right], \end{aligned}$$

approximation, Eq. (5), becomes

$$\Delta h = 2 \sqrt{\frac{2R_1R_2}{R_1 + R_2}} |\sin \theta|^{3/2} \sqrt{l}, \quad (10)$$

and the measure $M(l; R_1, R_2)$ of lines generating chords shorter than l is

$$M(l; R_1, R_2) = \int_{-\pi/2}^{\pi/2} \Delta h d\theta = 2 \sqrt{\pi} \frac{\Gamma\left(\frac{5}{4}\right)}{\Gamma\left(\frac{7}{4}\right)} \sqrt{\frac{2R_1R_2}{R_1 + R_2}} \sqrt{l}. \quad (11)$$

In the case of a general distribution of radii, we introduce the two quantities $\nu_c(R_1, R_2)$ and $g(R)$ defined as follows.

(a) $\nu_c(R_1, R_2) dR_2$ is the mean number of contact points between disks of radius R_1 and disks of radius between R_2 and $R_2 + dR_2$, per disk of radius R_1 (it corresponds to n_c in Sec. II).

(b) $g(R)$ is the density probability function of disks of radius R , normalized to unity. [We note that the two quantities are related by $\nu_c(R_1, R_2) g(R_1) = \nu_c(R_2, R_1) g(R_2)$.]

Furthermore, we denote by N the total number of disks of the system. With these notations, the measure of the set of lines giving a chord less than l is given by [such as in Eq. (5), the factor 1/2 is there because each point of contact is counted twice]

$$\frac{1}{2} \int \int M(l; R_1, R_2) \nu_c(R_1, R_2) dR_2 N g(R_1) dR_1. \quad (12)$$

The probability of generating such a chord is obtained by dividing Eq. (12) by the total number of chords, which is the total perimeter of the disks of the system:

$$\int_0^{+\infty} (2\pi R) N g(R) dR = 2\pi N \bar{R}, \quad (13)$$

where $\bar{R} = \int_0^{+\infty} R g(R) dR$ is the mean radius. Thus, using Eqs. (12) and (13) we obtain the distribution function of the chord length at small chords:

$$\begin{aligned} F(l) &= \frac{1}{2\sqrt{\pi}} \frac{\Gamma\left(\frac{5}{4}\right)}{\Gamma\left(\frac{7}{4}\right)} \frac{\sqrt{l}}{\bar{R}} \\ &\quad \times \left[\int \int \nu_c(R_1, R_2) \sqrt{\frac{2R_1R_2}{R_1 + R_2}} g(R_1) dR_1 dR_2 \right]. \end{aligned}$$

Thus, the density distribution function of chords for this system at small chords is

$$\begin{aligned} f(l) &= \frac{1}{4\sqrt{\pi}} \frac{\Gamma\left(\frac{5}{4}\right)}{\Gamma\left(\frac{7}{4}\right)} \frac{1}{\bar{R} \sqrt{l}} \\ &\quad \times \left[\int \int \nu_c(R_1, R_2) \sqrt{\frac{2R_1R_2}{R_1 + R_2}} g(R_1) dR_1 dR_2 \right]. \end{aligned} \quad (14a)$$

Note that Eq. (14a) reduces to Eq. (7) when $\nu_c(R_1, R_2)g(R_1) = n_c \delta(R - R_1) \delta(R - R_2)$. For general random packings $\nu_c(R_1, R_2)$ is unknown. However, if we consider a packing of disks of only two different radii, say r_1 and r_2 , distributed according to $g(R) = p \delta(r_1 - R) + (1 - p) \delta(r_2 - R)$ (p being the ratio of disks of radius r_1), we have

$$\begin{aligned} \nu_c(R_1, R_2)g(R_1) &= \nu_{11} \delta(r_1 - R_2) p \delta(r_1 - R_1) \\ &+ \nu_{22} \delta(r_2 - R_2) (1 - p) \delta(r_2 - R_1) \\ &+ \nu_{12} \delta(r_2 - R_2) p \delta(r_1 - R_1) \\ &+ \nu_{21} \delta(r_1 - R_2) (1 - p) \delta(r_2 - R_1), \end{aligned} \quad (14b)$$

where we have used the following notations;

$$\begin{aligned} \nu_{11} &= \nu_c(r_1, r_1), & \nu_{22} &= \nu_c(r_2, r_2), \\ \nu_{12} &= \nu_c(r_1, r_2), & \nu_{21} &= \nu_c(r_2, r_1). \end{aligned} \quad (14c)$$

Then, using Eqs. (14b) and Eq. (14c), Eq. (14a) simplifies to

$$\begin{aligned} f(l) &= \frac{1}{4\sqrt{\pi}} \frac{\Gamma\left(\frac{5}{4}\right)}{\Gamma\left(\frac{7}{4}\right)} \frac{1}{\bar{R}} \frac{1}{\sqrt{l}} \left[p \nu_{11} \sqrt{r_1} + (1 - p) \nu_{22} \sqrt{r_2} \right. \\ &\left. + [p \nu_{12} + (1 - p) \nu_{21}] \sqrt{\frac{2 r_1 r_2}{r_1 + r_2}} \right], \end{aligned} \quad (15)$$

where $\bar{R} = p r_1 + (1 - p) r_2$. This result will be tested for ordered packings through Monte Carlo simulations in the following section.

IV. MONTE CARLO SIMULATIONS

In this section, Monte Carlo simulations are performed for various disk packings and for isolated systems. The Monte Carlo program that generates random lines in the plane and then collects chords across the body has been described in Ref. [10]. It has been tested for various simple geometric objects where the CLD is known analytically [11], as well as for random media [10].

First, we have conducted the simulation for four different types of lattice of monodisperse unit radius disks.

(a) The square lattice and the hexagonal lattice where disks have been removed, shown in Fig. 4. Both packings have a coordination number of 4.

(b) The triangular lattice, where $n_c = 6$.

(c) The honeycomb lattice, where $n_c = 3$.

In any of the cases the simulations fit very well with the theoretical CLD given in Eq. (7) as illustrated in Figs. 4 and 5. The details of the different simulations are presented in Table I.

Then, we have tested the ordered packing of two kinds of disks generated in filling the interstices of a square lattice of

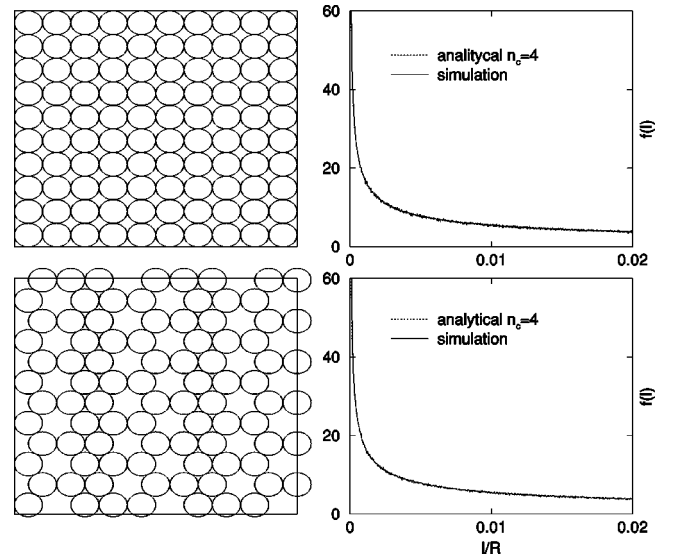


FIG. 4. Chord length distribution functions $f(l)$ vs dimensionless distance l/R for ordered packings, both system have the same coordination number $n_c = 4$ and the same analytical CLD near the origin.

unit disks by disks of radius $\sqrt{2} - 1$ (labeled lattice 1) as shown in Fig. 6.

The second packing tested (labeled lattice 2), shown in the same figure, is obtained from the former one by taking off one small disk out of two. The coordination numbers for these two packings are $\nu_{11} = \nu_{12} = \nu_{21} = 4$, $\nu_{22} = 0$ and $\nu_{11} = \nu_{21} = 4$, $\nu_{12} = 2$, $\nu_{22} = 0$ respectively. Simulations were performed for 20 000 and 15 000 disks; 10^5 lines were generated and more than 10×10^6 chords were collected in each case. Again, the simulation results fully correspond to the analytical prediction of Eq. (15).

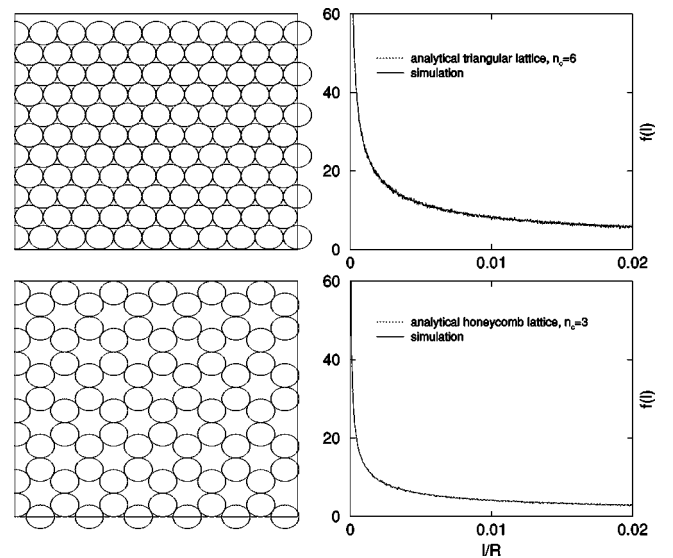


FIG. 5. Chord length distribution functions $f(l)$ vs dimensionless distance l/R for ordered hexagonal packings, first system is the hexagonal lattice or triangular lattice with $n_c = 6$, the second is the honeycomb lattice with $n_c = 3$.

TABLE I. Packing of monodisperse disks: simulation results.

	No. of disks	n_c	No. of lines	No. of chords	Simulation time ^a
Triangular lattice	11500	6	10^5	10.8×10^6	~ 20 min
Square lattice	10000	4	10^5	9.3×10^6	~ 24 min
Honeycomb lattice	8400	3	10^5	7.5×10^6	~ 22 min
Triangular lattice with holes	8950	4	10^5	8.2×10^6	~ 15 min
Ballistic packing	10371	4	10^6	97.0×10^6	~ 2 h 30 min
Packing on a plane	7494	~2.16 ^b	10^6	69.0×10^6	~ 1 h 48 min

^aOn a pentium IV at 3.06 GHz.

^bResults from simulations.

In order to study random disk packings, we use two ballistic deposition models in which spheres or disks are dropped from a random point above the bottom of the box (here a square for the spheres and a line segment for the disks) one after another [13,14]. Under the gravitational forces, the dropped particle will roll over the existing particles until it reaches a stable position. It is considered as a static model since once a ball finds a stable position it remains in place.

The first ballistic model we used is a pure two-dimensional ballistic deposition model in which the coordination number is known as 4 [15]. The second one is a three-dimensional one where spheres are dropped on a plane and we look at the pattern formed by these spheres in the horizontal plane at the height of the sphere's radius. The interest of the second model is that we free our system from gravitational effects, making it isotropic. However, to the best of our knowledge, the coordination number for this model is not known. In the first case, the simulation confirms the analytical value of $n_c=4$. There exists a little hump around the radius of 0.002 in Fig. 7, which is due to the inaccuracy of our deposition algorithm.

For the second model, the simulations show the expected behavior in $1/\sqrt{l}$ for the CLD, giving an experimental value for the coordination number of $n_c \approx 2.16$. This corresponds to an unjammed packing since a necessary condition for a particle to be jammed is that the particle must have, in two dimensions, at least three neighboring contacts not all in the same half circle [7]. This behavior in $1/\sqrt{l}$ of the CLD is also present for relatively long chords (up to 1.5 times the radius as we can see in Fig. 8). Note that we had to simulate up to 1×10^6 lines for this last model in order to get good statistics due to the existence of a more important void region, making possible the presence of long chords. Other irreversible-deposition models of spheres on a plane, such as models that interpolate between random sequential adsorption model and ballistic deposition model [16] can be studied in the same way.

Finally, we tested the isolated system of two touching disks. We generated 20×10^6 straight lines; 7.2×10^6 chords were collected in the case where $R_1=R_2=1$ and 5.6×10^6 chords in the case where $R_1=3$ and $R_2=1$. Each simulation takes less than 4 min on a pentium IV at 3.06 GHz. The simulations presented in Fig. 9 fit very well with the theoretical predictions given by Eqs. (A5a) and (A5b).

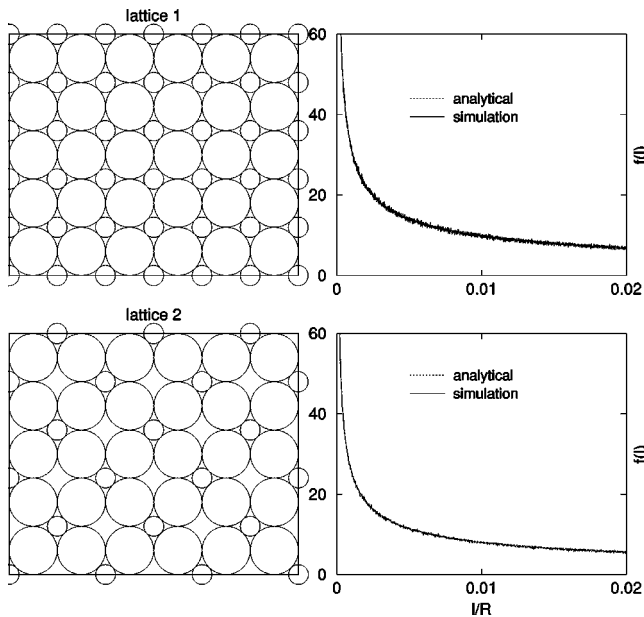


FIG. 6. Chord length distribution functions $f(l)$ vs dimensionless distance l/R for two packings of two kinds of disks.

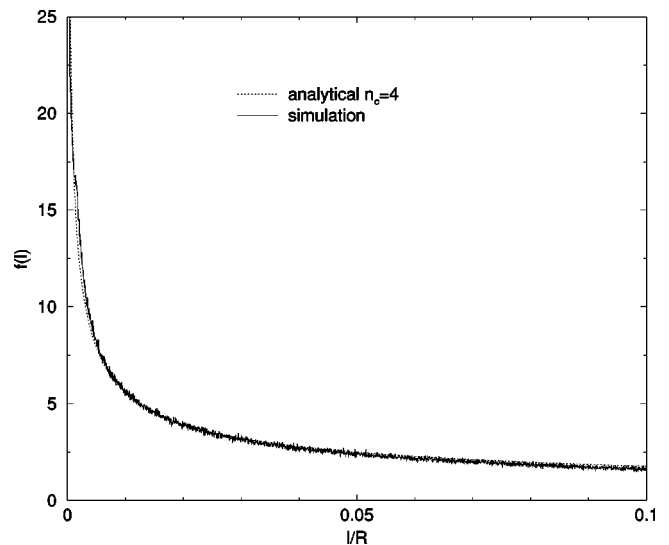


FIG. 7. Chord length distribution functions $f(l)$ vs dimensionless distance l/R for a random packing of disks built by the ballistic deposition algorithm.

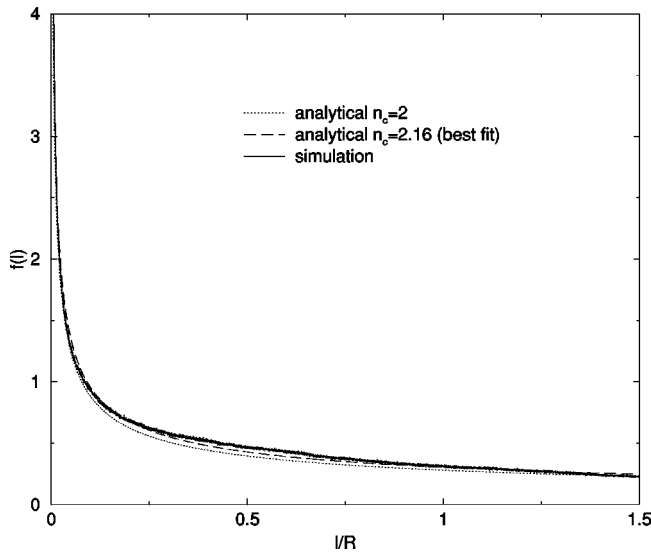


FIG. 8. Chord length distribution functions $f(l)$ vs dimensionless distance l/R for a random packing of disks on a plane.

V. DISCUSSION

In this section we focus on random packings of equal disks. Based on pure geometric argument, we have derived a general formula, Eq. (7), for the chord length distribution of an assembly of random equal touching disks that depends only on the coordination number. Torquato and co-workers [6,17,18], using techniques arising from statistical physics (scaled-particle theory) derived the expression of the CLD for a statistically isotropic random packing of mono or poly-disperse n -dimensional spheres. Their results for a random packing of equal disks are the following:

$$p(l) = \frac{2\eta}{\pi(1-\eta)R} \exp\left[-\frac{2\eta}{\pi(1-\eta)} \frac{l}{R}\right]. \quad (16)$$

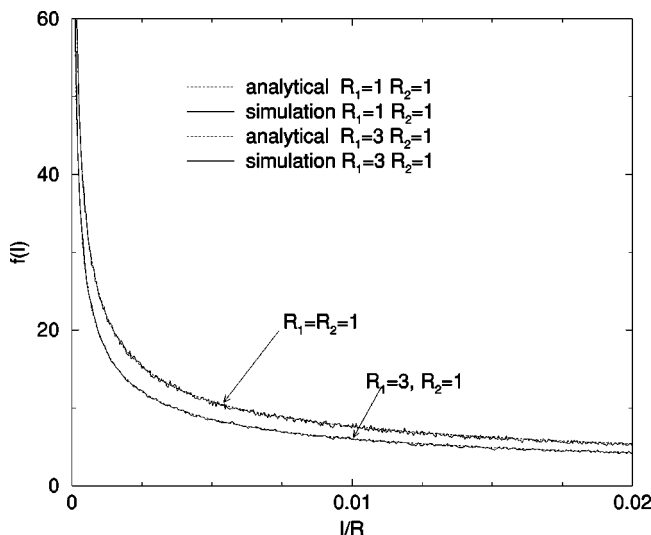


FIG. 9. Chord length distribution functions $f(l)$ vs dimensionless distance l/R for a system consisting of two isolated disks in contact.

This result, which depends only on the packing fraction η , is in apparent contradiction with the result obtained in Eq. (7) for small chords. However, Torquato’s results are obtained for systems at complete unconstrained equilibrium where complete equilibrium means that statistical averages are taken over all configurations limited only by the principle of no overlap. Such averages correspond to the full thermodynamic state of the hard disk system [19]. This hypothesis is not verified for the ballistic deposition models we used in Sec. IV where disks are frozen as soon as they find a stable position or hit the ground. Indeed, the distribution of the CLD at small distances is governed by n_c , the mean number of contacts. Our calculations assumed implicitly n_c to be nonzero. Torquato’s results thus correspond to a null value of n_c , which accounts for the absence of the divergence for small chords. In fact, it is known that disordered equilibrium hard disk systems are only “jammed” (i.e., disks are in contact) at a special singular point known as the maximally random jammed state [20]. For a two phase random media, Lu and Torquato [18] also introduce a useful statistical measure $L^i(z)$ called the lineal-path-function, which is defined for statistically isotropic media as the probability that a line segment of length z lies wholly in phase i when randomly thrown into the sample. Here, since we only consider the vacuum, we drop index i and $L(z)$ always refers to the phase outside the disks. Note that $L(z)$ is a probability and not a probability density. Using a simple probabilistic argument these authors show that $L(z)$ is related to the usual chord length probability density function in the vacuum f by

$$L(z) = \phi \frac{\int_0^\infty \Theta(y-z)(y-z)f(y) dy}{\int_0^\infty y f(y) dy}, \quad (17)$$

where $\Theta(x)$ is the Heaviside step function and $\phi=1-\eta$ is the void fraction. Our result concerning the CLD at small chords, Eq. (7), allows us to determine $L(z)$ for small values of z . First note that the denominator in Eq. (17) is just the mean chord length \bar{l} and is given by Cauchy’s theorem in two dimensions,

$$\bar{l} = \int_0^\infty y f(y) dy = \pi \frac{\phi}{s}, \quad (18)$$

where s is the specific length, i.e., the interface length per unit surface. For random disk packings, the vacuum phase has a nonconvex shape that might even be nonconnex. However, even for nonconvex shapes Cauchy’s theorem remains valid [12]. The numerator in Eq. (17) is,

$$\int_z^\infty (y-z)f(y) dy = \bar{l} - z - \int_0^z (y-z)f(y) dy, \quad (19)$$

using Eq. (7) for evaluating the integral on the right-hand side of Eq. (19) gives, for small z ,

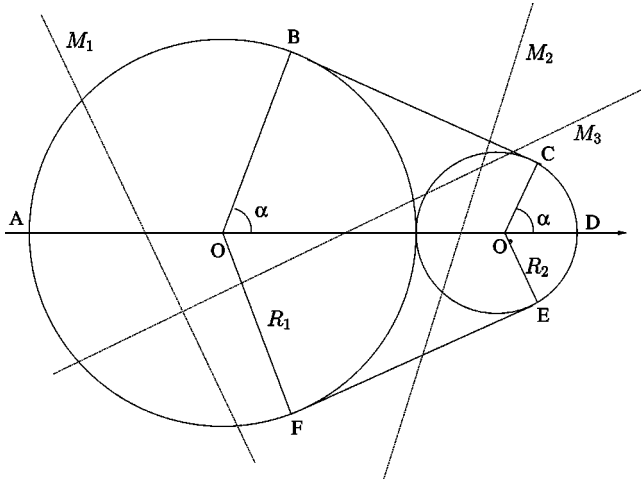


FIG. 10. Isolated disks: random line M_1 or M_2 do not generate any chord, M_3 generates one chord. $[ABCDEF]$ is the outer cover or convex hull of the system.

$$\int_0^z (y-z) f(y) dy = -\frac{n_c}{3\sqrt{\pi R}} \frac{\Gamma\left(\frac{5}{4}\right)}{\Gamma\left(\frac{7}{4}\right)} z^{3/2}. \quad (20)$$

Using Eqs. (18)–(20) in Eq. (17) leads to

$$L(z) = \phi \left[1 - \frac{z}{l} + \frac{n_c}{3\sqrt{\pi R}} \frac{\Gamma\left(\frac{5}{4}\right)}{\Gamma\left(\frac{7}{4}\right)} \frac{z^{3/2}}{l} \right]. \quad (21)$$

The last term in Eq. (21) is a correction to $L(z)$ at small z due to the specific geometry of the system. Note that for $z = 0$ we recover $L(0) = \phi$, i.e., the probability of having a random point in the vacuum is ϕ . The first two terms are independent of the geometry of the system and are obtained from simple probabilistic arguments in Appendix B.

ACKNOWLEDGMENT

It is a pleasure to thank Benoît Roesslinger for reading the manuscript and for his comments.

APPENDIX A: CHORD LENGTH DISTRIBUTION FOR TWO ISOLATED DISKS

In this appendix, we derive the CLD for a couple of two isolated touching disks. For such a system the CLD normalization needs special care. Indeed, the measure of random lines defined in Sec. II by Eq. (1) overestimates the number of chords since for an isolated system some lines do not generate any chord, as shown in Fig. 10.

Consequently, the measure of chords must be normalized according to the number of random lines that cut both disks D_1 and D_2 , which is formally

$$\int_{\substack{M \cap D_1 \neq \emptyset \\ M \cap D_2 \neq \emptyset}} dM, \quad (A1)$$

where dM is the density of random lines across an object defined by Eq. (1). Matai [9] gives a derivation of this geometric problem for convex bodies in the plane and the result is the following:

$$\int_{\substack{M \cap D_1 \neq \emptyset \\ M \cap D_2 \neq \emptyset}} dM = L_1 + L_2 - L_{12}, \quad (A2)$$

where L_1 and L_2 are the perimeters of the disk D_1 and D_2 , respectively, and L_{12} is the perimeter of the outer cover or convex hull $[ABCDEF]$ of D_1 and D_2 (see Fig. 10). Consequently, the distribution function of chords for the isolated system $F_{is}(l)$ is

$$F_{is}(l) = \frac{\int_{-\pi/2}^{\pi/2} \Delta h d\theta}{L_1 + L_2 - L_{12}}, \quad (A3)$$

where Δh is given by Eq. (10). Performing the integration over θ and the derivative with respect to l leads to

$$f_{is}(l) = \frac{\sqrt{\pi}}{L_1 + L_2 - L_{12}} \sqrt{\frac{2R_1 R_2}{R_1 + R_2}} \frac{\Gamma\left(\frac{5}{4}\right)}{\Gamma\left(\frac{7}{4}\right)} \frac{1}{\sqrt{l}}, \quad (A4)$$

for the chord length distribution of two isolated disks at small lengths. Since L_{12} is given by (see Fig. 10)

$$L_{12} = 2[2\sqrt{R_1 R_2} + \pi R_1 + (R_2 - R_1)\alpha]$$

$$\text{with } \alpha = \arccos\left(\frac{R_1 - R_2}{R_1 + R_2}\right),$$

Eq. (A4) is finally,

$$f_{is}(l) = \frac{\sqrt{\pi}}{2\pi R_2 - 4\sqrt{R_1 R_2} + 2(R_1 - R_2)\alpha} \times \sqrt{\frac{2R_1 R_2}{R_1 + R_2}} \frac{\Gamma\left(\frac{5}{4}\right)}{\Gamma\left(\frac{7}{4}\right)} \frac{1}{\sqrt{l}}. \quad (A5a)$$

For the special case of two equal disks, the preceding equation simplifies to

$$f_{is}(l) = \frac{\sqrt{\pi}}{2(\pi - 2)\sqrt{R}} \frac{\Gamma\left(\frac{5}{4}\right)}{\Gamma\left(\frac{7}{4}\right)} \frac{1}{\sqrt{l}}. \quad (A5b)$$

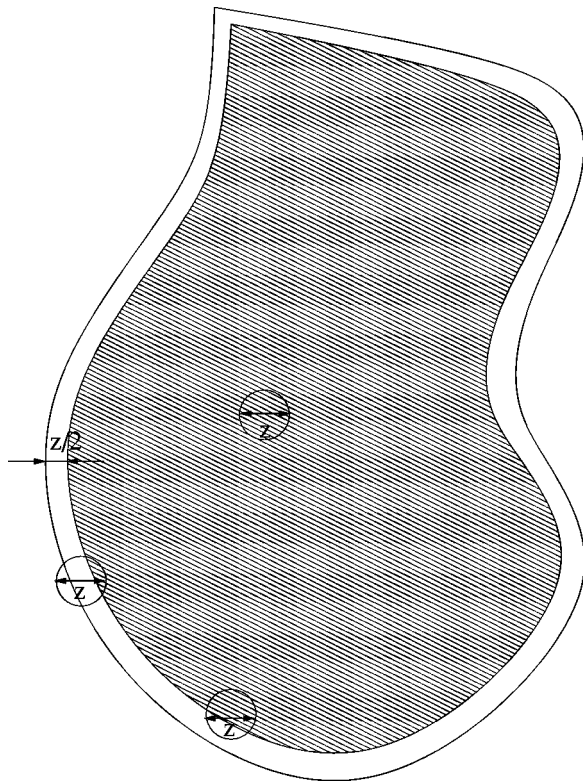


FIG. 11. Calculation of the lineal path function near the origin.

APPENDIX B: LINEAL PATH FUNCTION NEAR THE ORIGIN

Recall that the lineal path function for a phase is defined as the probability that a line segment of length z lies wholly in the phase when randomly thrown into the sample. This definition is valid for statistically isotropic media. Now consider a phase satisfying the preceding assumptions. This phase may be convex, nonconvex, or even nonconnex and has a filling fraction ϕ . Throwing a line segment of length z at random in the medium is a three-step process: (i) first, choose a special point on the line (say the middle); (ii) then, locate it uniformly in the sample; and (iii) finally, choose a random orientation for the segment.

Once the randomly chosen segment center is in the phase considered (with probability ϕ), two different cases can occur.

(1) The segment's center is at a distance x smaller than $z/2$ from the interface.

(2) The segment's center is at a distance greater than $z/2$ from the interface.

In the last eventuality, the segment's center is inside the hatched area whose surface is, for small z , $S - Lz/2$ (where S and L are the area and perimeter of the phase considered, see

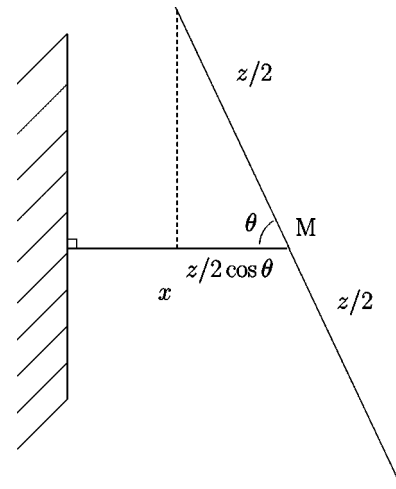


FIG. 12. Random segment near the interface.

Fig. 11) and the whole segment is within the phase considered.

In the first case, the probability for the segment to hit the interface, knowing that the segment's center is at a distance x from the interface is, at the first order,

$$\int_{-\theta_0}^{\theta_0} \frac{d\theta}{\pi} = \frac{2\theta_0}{\pi}, \tag{B1}$$

where $\theta_0 = \arccos(2x/z)$ (see Fig. 12) and θ has been taken with uniform density in $[-\pi/2, \pi/2]$.

Thus the probability of hitting the interface knowing that the segment's center lies in the phase at a distance smaller than $z/2$ from the interface is

$$\int_0^{z/2} \frac{dx}{z/2} \frac{2\theta_0}{\pi} = \frac{4}{\pi z} \int_0^{z/2} \arccos\left(\frac{2x}{z}\right) dx = \frac{2}{\pi}, \tag{B2}$$

where x has been taken with uniform density in $[0, z/2]$. Consequently, the conditional probability $L(z)$ around the origin is

$$\begin{aligned} L(z) &= \phi \left[\left(S - L \frac{z}{2} \right) \frac{1}{S} + \left(1 - \frac{2}{\pi} \right) \left(L \frac{z}{2} \right) \frac{1}{S} \right] \\ &= \phi \left[1 - \frac{zL}{\pi S} \right] \\ &= \phi \left[1 - \frac{z}{\bar{l}} \right], \end{aligned} \tag{B3}$$

which is the beginning of the development of Eq. (21). It is also interesting to note that the slope of the lineal path function is $-\phi/\bar{l}$ at the origin.

[1] T.I. Quickenden and G.K. Tan, *J. Colloid Interface Sci.* **48**, 236 (1974).
 [2] J. Serra, *Image Analysis and Mathematical Morphology* (Academic Press, London, 1982).

[3] T.J. Donovan and Y. Danon, *Nucl. Sci. Eng.* **143**, 226 (2003).
 [4] Y. Pomeau, *Ann. Inst. Henri Poincaré* **38**, 75 (1983).
 [5] Y. Pomeau and J. Serra, *J. Microsc.* **138**, 179 (1985).
 [6] S. Torquato, *Random Heterogeneous Materials: Microstruc-*

- ture and Macroscopic Properties* (Springer-Verlag, New York, 2002).
- [7] S. Torquato and F.H. Stillinger, *J. Phys. Chem. B* **105**, 11 849 (2001).
- [8] L. A. Santaló, *Integral Geometry and Geometric Probability* (Addison-Wesley, Reading, MA, 1976).
- [9] A. M. Matai, *An Introduction to Geometrical Probability* (Gordon and Breach Science, Amsterdam, 1999).
- [10] A. Mazzolo and B. Roesslinger, in Proceedings of the IV IMACS Seminar on Monte Carlo Methods, 2003, Berlin, special issue of Monte Carlo Methods and Applications (to be published).
- [11] A. Mazzolo, B. Roesslinger, and C.M. Diop, *Ann. Nucl. Energy* **29**, 1391 (2003).
- [12] A. Mazzolo, B. Roesslinger, and W. Gille, *J. Math. Phys.* **44**, 6195 (2003).
- [13] W.H. Visscher and H. Bolterlii, *Nature (London)* **239**, 504 (1972).
- [14] A. Pavlovitch, R. Jullien, and P. Meakin, *Physica A* **176**, 206 (1991).
- [15] D. Bideau, A. Gervois, L. Oger, and J.P. Troadec, *J. Phys. (Paris)* **47**, 1697 (1986).
- [16] G. Tarjus, P. Viot, H.S. Choi, and J. Talbot, *Phys. Rev. E* **49**, 3239 (1994).
- [17] S. Torquato and B. Lu, *Phys. Rev. E* **47**, 2950 (1993).
- [18] B. Lu and S. Torquato, *Phys. Rev. A* **45**, 922 (1992).
- [19] H. Reiss, H.M. Ellerby, and J.A. Manzanares, *J. Chem. Phys.* **100**, 5970 (1996).
- [20] S. Torquato, T.M. Truskett, and P.G. Debenedetti, *Phys. Rev. Lett.* **84**, 2064 (2000).